Pre-print
Science of the Total Environment 741: 140461 (2020)

Bacterial ecotoxicity and shifts in bacterial communities associated with the removal of ibuprofen, diclofenac and triclosan in biopurification systems

Inés Aguilar-Romero, Esperanza Romero, Regina-Michaela Wittich, and Pieter van Dillewijn*

Department of Environmental Protection. Estación Experimental del Zaidín - Consejo Superior de Investigaciones Científicas (EEZ-CSIC). Calle Profesor Albareda 1, 18008 Granada, Spain.

E-mail addresses: ines.aguilar@eez.csic.es (I. Aguilar-Romero), esperanza.romero@eez.csic.es (E. Romero), rwittich@eez.csic.es (R.-M. Wittich), pieter.vandillewijn@eez.csic.es (P. van Dillewijn).

* Corresponding author: pieter.vandillewijn@eez.csic.es

Abstract

The proliferation and possible adverse effects of emerging contaminants such as pharmaceutical and personal care products (PPCPs) in waters and the environment is causing increased concern. We investigated the dissipation of three PPCPs: ibuprofen (IBP), diclofenac (DCF) and triclosan (TCS), separately or in mixture, in the ppm range in microcosm biopurification systems (BPS), paying special attention to their effect on bacterial ecotoxicity and on bacterial community structure and composition. The results reveal that the BPS efficiently dissipates IBP and DCF with 90% removal after 45 and 84 days of incubation, respectively. However, removal of TCS required longer incubation, 127 days for 90% removal. Furthermore, dissipation of the three PPCPs was slower when all three were applied to the BPS as a mixture. TCS had an initial negative effect on bacterial viability by a decrease of 34-43%; however, this effect was mitigated when all three PPCPs were present simultaneously. The bacterial communities in the BPS were affected much more by incubation time than by the applied PPCPs. Nonetheless, the PPCPs affected differentially the composition and relative abundance of bacterial taxa. IBP and DCF initially increased bacterial diversity and richness while exposure to TCS generally provoked the opposite effect. TCS had the largest effect on bacterial groups negatively affecting the relative abundance of *Acidobacteria, Rickettsiales*, *Methylophilales, Methylacidiphilae* and *Phycisphaerae.* On the other hand, all three PPCPs stimulated the dominant bacterial families *Promicromonosporaceae, Caulobacteraceae, Xanthomonadaceae, Cyclobacteriaceae, Sphingobacteriaceae* and *Verrucomicrobiaceae*, whose members could harbour mechanisms for resistance by degradation and/or detoxification.

Keywords: (max 6) PPCPs, endocrine disruptors, bacterial community, ecotoxicity, biopurification systems

Abbreviations:

PPCPs: Pharmaceuticals and Personal Care Products

ppm: parts per million

ppb: parts per billion

IBP: ibuprofen

DCF: diclofenac

TCS: triclosan

BPS: Biopurification system

WWTP: Wastewater treatment plants

RA: relative abundance

1. Introduction

Pharmaceuticals and personal care products (PPCPs) used as medicinal drugs or to improve the quality of daily life, are being considered emerging contaminants of public concern. PPCPs are increasingly being detected in the aquatic environments, such as water, sediment and biota (Ebele et al., 2017; Peng et al., 2019). The presence of PPCPs in surface water may have negative ecological impacts even at low concentrations, due to their continuous introduction into environments through different anthropogenic sources (Houtman, 2010; Ebele et al., 2017). In rural areas with low population densities, untreated sewage is directly discharged into the sea or rivers (Daughton and Ternes, 1999). However, effluents from wastewater treatment plants (WWTP) are the main route of entry of PPCPs into the aquatic environment (Petrović et al., 2003; Castiglioni et al., 2005; Rosal et al., 2010). Among PPCPs, two non-steroidal anti-inflammatory drugs: ibuprofen (IBP) and diclofenac (DCF), and the antimicrobial agent triclosan (TCS) are commonly detected in surface water at concentrations of ng per litre (ppb) (Wilkinson et al., 2017). These contaminants have been shown to pose harmful effects on aquatic organisms such as fish, algae and invertebrates (Lonappan et al., 2016; Olaniyan et al., 2016). Moreover, TCS which has been detected in drinking water and in plants cultivated in soils amended with biosolids from WWTPs, or irrigated with sewage, is an important risk for human health because it can cause endocrine disruption and affect different tissues (Gee et al., 2008; Jung et al., 2012; Geens et al., 2012). Therefore, the development of an appropriate technology is required that allows the efficient removal of PPCPs before effluent discharge (Grassi et al., 2013).

Bioremediation strategies include biopurification systems (BPS), also known as biobeds, which have been used successfully on-farm to remove organic pollutants from

84 wastewaters, and are being implemented as a system to control point-source
85 contamination (De Wilde et al., 2007; Castillo et al., 2008; Dias et al.,, 2020; Karas et
86 al., 2016). The main substrate of BPS is a biomixture of topsoil and organic materials
87 which harbours indigenous microorganisms which can become adapted to eliminate
88 these pollutants (Castillo Diaz et al., 2016; Aguilar-Romero et al., 2019). Recently,
89 Delgado-Moreno et al. (2019) suggested that BPS based on a biomixture composed of
90 agro-industrial olive oil waste, as available and sustainable local organic materials,
91 could be a workable strategy to remove PPCPs from wastewaters generated by the
92 pharmaceutical industry, hospitals, or effluents from wastewater treatment plants.

93 As has been documented, the efficiency of the BPS to remove contaminants such as
94 pesticides must be ascribed to the functioning and resilience of the microbial
95 communities of the BPS (Marinozzi et al., 2013; Tortella et al., 2013; Dealtry et al.,
96 2016; Castro-Gutiérrez et al., 2017; Diez et al., 2017, 2018; Holmsgaard et al., 2017; El
97 Azhari et al., 2018; Góngora-Echeverría et al., 2018). However, little is known
98 regarding the impact of PPCPs on the microbial population of this system. The current
99 study investigates the potential removal of three PPCPs, alone and in mixture, in BPS
100 microcosms; how interactions between contaminants can affect their dissipation
101 kinetics, their possible toxic effects on the indigenous microbial community of the BPS,
102 as well as the principal bacterial groups potentially involved in the bioremoval of these
103 PPCPs.

104 **2. Materials and methods**

105 *2.1 Chemicals*

106 Ibuprofen (IBP) (≥ 98% purity), diclofenac sodium salt (DCF) (≥ 98.5% purity) and
107 triclosan (TCS) (> 97% purity) were purchased from Sigma-Aldrich (Steinheim,

Germany). HPLC-grade solvents from Scharlau (Barcelona, Spain) and MilliQ water were used.

2.2 Degradation study in BPS microcosms

Biopurification systems (BPSs) were constructed at microcosm scale with a biomixture containing an agricultural silty clay loam soil, vermicompost of wet olive cake and olive tree prunings (1:1:2, v:v:v). Physicochemical properties of the biomixture were described by Delgado-Moreno et al. (2019). Each BPS was prepared in triplicate and the biomixture contaminated with either 100 μg g^{-1} of IBP, 20 μg g^{-1} of DCF or 20 μg g^{-1} of TCS, or all together as a mixture. The quantity of IBP was 5 times higher than the other compounds due to its reported fast dissipation in BPS (Delgado-Moreno et al., 2019). For this purpose, 1 g of silica sand placed in a 200 mL glass container used to house the microcosms was spiked with a solution of acetone containing each compound, either separately or as a mixture. After solvent evaporation, 60 g of the biomixture was added and mixed in an end-over-end rotary shaker for 15 min at room temperature. The biomixtures were moistened to 75% of their field capacity and the microcosms were incubated in darkness in a thermostatic chamber at 20ºC. The moisture content was maintained by adding sterile distilled water weekly. Autoclaved biomixtures were prepared in parallel as an abiotic control as described by Aguilar-Romero et al. (2019). BPSs with non-contaminated biomixtures were run in parallel to determine the effect caused by experimental conditions on the microbial populations. For work-up, the PPCPs were extracted at 0, 7, 14, 21, 50 and 79 days from 3 g (dry-weight) of biomixture by adding 6 ml of acetonitrile acidified with 1% acetic acid and vortexing for 1 min. Then, 1 g of a salts mixture (QuEChERS EN Pouch, Agilent Technologies, Santa Clara, CA, USA) was added and vortexed again for 1 min. Samples were

centrifuged for 5 min at 3500 rpm, filtered with a 0.45 µm PTFE filter and analysed by high-performance liquid chromatography (HPLC, series 1100 system, Agilent Technologies), using the conditions described by Delgado-Moreno et al. (2019). The extraction method recoveries for IBP, DCF and TCS were 87%-92%, 82%-90% and 82%-106%, respectively (Delgado-Moreno et al., 2019).

2.3 Total DNA isolation and amplicon sequencing analysis

To determine the effect of PPCPs on the indigenous bacterial community, total genomic DNA was extracted from 0.5 g (wet weight) of biomixture from each microcosm-scale BPS at different times using the FastDNA® Spin Kit for soil (MP Biomedicals, Solon, OH, USA). The DNA was quantified by using the Qubit dsDNA BR Assay kit (Live Technologies, Invitrogen, USA). Then, DNA samples were submitted for high-throughput 16S rRNA gene amplicon sequencing to Integrated Microbiome Resource (www.cgeb-imr.ca, Halifax, Nova Scotia, Canada). Primers for the V4-V5 variable regions of the 16S rRNA gene (Walters et al., 2015) were used and the amplified products were sequenced with Illumina MiSeq using 2 x 300 bp PE v3 chemistry (Comeau et al., 2017). All sequence files were submitted to the National Center for Biotechnology Information (NCBI) Sequence Read Archive (SRA - https://www.ncbi.nlm.nih.gov/sra) and are accessible in BioProject PRJNA603893.

2.4 Bioinformatic data analysis

Bacterial 16S V4-V5 region sequences were processed using QIIME version 1.9.0 (Caporaso et al., 2010b). Forward and reverse sequences were joined, fastq files were filtered for quality (Phred 20) and potential chimeras were detected and removed from the dataset using usearch61 (Edgar et al., 2011). The remaining sequences were clustered into Operational Taxonomic Units (OTUs) at 97% similarity level following

156 an open reference OTU picking strategy using UCLUST (Edgar et al., 2011).
157 Representative sequences of each OTU were aligned against SILVA database (v132;
158 (Quast et al., 2013)) using PyNAST (Caporaso et al., 2010a).

159 *2.5 Real-Time PCR quantification (qPCR)*

160 The total bacterial community and the abundance of *Acidobacteria* and *Alpha-, Beta-*
161 and *Gammaproteobacteria* were quantified by real-time PCR assays using the taxon-
162 specific 16S rRNA primers and thermal conditions described by Philippot et al. (2011).
163 The real-time PCR reactions were carried out in 12.5 µl of volume using 6.25 µl of
164 iQ™ SYBR® Green Supermix (Bio-Rad Laboratories, Hercules, CA, USA), 400 nM of
165 each primer and 1 ng of DNA. All samples were run in triplicate. Serial dilutions of
166 linearized pCR2.1-TOPO® containing cloned sequences of the 16S rRNA gene specific
167 for each taxa were used for standard curves. The PCR efficiency values ranged between
168 81 and 103%. To check for the presence of inhibitors in the DNA used for qPCR assays,
169 DNA samples from biomixtures were mixed with a known amount of standard DNA
170 prior to qPCR. No inhibitors were detected in the assays.

171 *2.6 Toxicological study*

172 To determine the toxic effects of PPCPs on the microbial populations, the number of
173 live microorganisms was determined in non-sterile samples at different times by
174 microscopic analyses using the LIVE/DEAD® BacLight™ Bacterial Viability Kit
175 (Molecular Probes®, Life Technologies, USA). For this purpose, the microorganisms
176 from 0.5 g of biomixture treated or not with PPCPs were extracted in 50 ml of
177 phosphate buffered saline (PBS) during 1 h by shaking at 30ºC in triplicate. Then, a
178 double concentrated working solution of the LIVE/DEAD BacLight staining reagent
179 mixture was prepared following the manufacturer's indications and mixed with an equal

180 volume of the bacterial suspension. This mixture was incubated at room temperature in
181 the dark for 15 minutes. Cell counts were performed from 10 µl with the aid of a
182 Neubauer chamber.

183 *2.7 Data modeling and statistical analysis*

184 To obtain the dissipation kinetics of the PPCPs in non-sterile samples, the single first-
185 order model ($C_t = C_0 \times e^{-kt}$) was tested using the modeling program Modelmaker 4.0
186 (Cherwell Scientific Ltd., Oxford, UK). C_0 and C_t indicate the concentration (µg g^{-1}) of
187 PPCPs at the initial time and time *t* (days), respectively, and *k* is the dissipation rate
188 constant ($days^{-1}$). The chi-square (χ^2) and scaled error values were used as criteria to
189 ensure that the theoretical kinetics fit experimental data.

190 Alpha diversity (Chao1, Shannon diversity index and Simpson's Evenness), and the
191 rarefaction curves of observed OTUs were determined using QIIME based on data
192 rarefied to the number of reads found in the least abundant sample. Similarly, QIIME
193 was used to perform principal component analysis (PCoA) based on Bray-Curtis
194 distances and PERMANOVA. Non-metric Multidimensional Scaling (NMDS)
195 ordination and hierarchical cluster analysis of bacterial community composition at the
196 phylum level based on the Bray-Curtis similarity index and the percentage of similarity
197 between means of groups of samples (n=3) using the Unweighted Pair Group Method
198 with Arithmetic mean (UPGMA) were determined using PAST software version 3.21
199 (https://folk.uio.no/ohammer/past/). For these analyses, outlier sample of biomixture 2
200 contaminated with triclosan at 7 days, T27, was not taken into account. SPSS Statistical
201 Software Package version 25 (IBM Corporation, New York, USA) was used for one-
202 way ANOVA at a significance level of 0.05.

203

3. Results and discussion

3.1 PPCP removal in BPS microcosms

To determine how PPCPs affect indigenous microbial populations in BPS, the disappearance of each compound was measured along time in BPS microcosms treated with IBP, DCF, or TCS, individually or simultaneously. The dissipation curves of the PPCPs are shown in Fig. 1. The single first-order model, except in the sterile controls, accurately fitted all the experimental data showing low chi-square and scaled error values ($\chi_{5,0.05}^2 = 11.070$, $err_{scaled} < 6.24$). The R^2 values were over 0.92, except for TCS (Table 1). Ibuprofen showed the highest dissipation rate constant *k*, with 100% being removed after 79 days of incubation, although the initial concentration of IBP in the BPS was 5 fold higher than that of the other compounds. DCF and TCS dissipated more slowly than IBP and required 84 and 127 days, respectively, for 90% removal (DT_{90}) when applied individually. The dissipation of IBP, DCF and TCS was even slower (DT_{90} 47, 137 and 180 days respectively), when applied simultaneously. In fact, in all cases *k* values were higher when the PPCPs were applied separately than as a mixture (Table 1). However, the difference in this increase was only statistically significant in samples contaminated with DCF (ANOVA, $p = 0.012$). This indicates that DCF removal in the BPS microcosms was affected by the presence of either TCS, IBP or by both. Likely, this could be attributed to the negative effect these compounds may have on groups of microorganisms implicated in DCF dissipation. According to the results obtained by Delgado-Moreno et al. (2019) where the three PPCPs were applied as a mixture, the dissipation rates for DCF and TCS were 3 and 2 fold higher, respectively, than the values obtained in this study. Nevertheless, the amount of IBP applied in this study was 5 fold higher, which could cause a negative effect on the microbial

228 populations harboured in the biomixtures which are responsible for DCF and TCS
229 dissipation. Another reason could be the existence of microorganisms with the ability to
230 transform more than one of the compounds but which exhibit substrate preferences. For
231 instance, Lu, Z. et al. (2019) reported that the bacterial strain *Pseudoxanthomonas* sp.
232 DIN-3, which has the ability to remove DCF, IBP, and Naproxen (each at 50 μg/L),
233 more effectively eliminated IBP than the other compounds in mixtures.
234 On the other hand, the results from the sterilized control treatments revealed that, after
235 79 days of incubation, the amounts of IBP, DCF and TCS which had disappeared were
236 47.6, 7.3 and 13.43%, respectively (Fig. 1). These percentages indicate that some
237 abiotic dissipation occurs, especially in microcosms treated with IBP. Under these
238 conditions, the removal of PPCPs could be influenced by the presence of clay particles
239 and solar radiation via photochemical reactions generating metabolites (Aranami and
240 Readman, 2007; Lonappan et al., 2016; Maldonado-Torres et al., 2018). In fact, two
241 likely abiotically formed metabolites of IBP and DCF, 1-(4-isobutylphenyl)ethanone
242 and 2-(9H-carbazol-1-yl) acetic acid, respectively, were detected in the same type of
243 BPS in a previous study (Delgado-Moreno et al., 2019).

244 *3.2. Bacterial community structure, dynamics and composition in the BPS microcosms*
245 To determine the response of bacterial communities to the PPCPs in the BPS
246 microcosms, amplicon products of the V4-V5 variable regions of the 16S rRNA gene
247 were analysed at different times. A total of 1,024,229 sequences were obtained after
248 quality filtering and the removal of possible chimera sequences. The depth of
249 sequencing of these samples was sufficient to cover the full diversity as indicated by
250 rarefaction curves (Fig. S1A).

3.2.1. Bacterial richness and diversity in the BPS microcosms

The diversity of the bacterial community in the BPS microcosms was determined over 50 days (Table 2). In the control BPS, the bacterial richness (chao1), the number of observed OTUs, the Shannon diversity and the Simpson's Evenness generally increased along the time with a dip at 7 to 14 days before increasing until the end of the incubation period at 50 days. Similar tendencies were observed in the BPSs exposed to PPCPs but with punctually significant differences with respect to the control. After 7 days, the BPSs exposed to IBP and DCF showed significantly higher diversity and evenness. After 14 days, specifically for IBP, the richness, diversity and evenness were significantly higher than in the control. Generally, both IBP and DCF give values for richness and diversity indices higher than the control. After 50 days, the number of observed OTUs and Shannon diversity for DCF were significantly higher. Jiang et al. (2017) also observed increased Shannon diversity in sequence batch reactors exposed to IBP and/or DCF after 130 days, indicating the resilience potential of the bacterial community in response to these two non-steroidal anti-inflammatory drugs at low concentrations. In TCS-exposed BPSs, the alpha diversity parameters compared to the control were significantly reduced after 50 days (Table 2). This indicated clearly that TCS negatively affects richness and diversity of the bacterial populations of the BPS. Recent studies have demonstrated that TCS is an environmental stressor, alters the community structure and reduces species diversity and richness (Clarke et al., 2019; Oh et al., 2019; Peng et al., 2019). The simultaneous treatment with the three PPCPs gave alpha diversity values generally lower than those obtained for IBP and DCF, and higher than for TCS alone, but not significantly different from the controls, except for a higher evenness after 7 days. Therefore, the negative impact generated by TCS on its own may

be compensated by the increase in richness and diversity caused by DCF, and especially IBP. With regard to other BPS studies, increased pesticide application was shown to decrease bacterial diversity in some (Holmsgaard et al., 2017), but in others the introduced pesticides had little or transient effects (Marinozzi et al., 2013; Tortella et al., 2013; Castrro-Gutierrez et al., 2017; Diez et al., 2017, 2018; Góngora-Echeverría et al 2018; El Azhari et al 2018). These results indicate that certain pesticides had concentration-dependent effects, but mostly that BPS bacterial communities were resilient to these types of contaminants.

3.2.2. Bacterial community structure and composition in the BPS microcosms

The bacterial community in all the BPS microcosms was composed of 38 different phyla, 10 of which comprised 98-99% of the total OTUs detected (Fig. 2A). *Proteobacteria* was the most abundant phylum (38.6-57.5%), followed by *Bacteroidetes* (13.5-48.4%), *Actinobacteria* (3.6-11.2%), *Planctomycetes* (3.1-9.4%), *Acidobacteria* (0.7-6.4%) and *Verrumicrobia* (0.3-5.6%). Hierarchal clustering analysis of the bacterial community composition along the time grouped the bacterial communities mainly according to the contaminant applied (Fig. 2B). The main cluster showed 82% similarity between microcosms treated with DCF and the other treatments. Within this cluster, BPS microcosms treated with IBP presented a cluster of high similarity (87%) with control microcosms at 21, 28 and 50 days, while those contaminated with TCS clustered more closely with those treated simultaneously with the three PPCPs (especially at 21, 28 and 50 days). Within each subcluster, the bacterial communities at initial times (7 and 14 days) group together in all cases.

Principal component analyses shows that 31.63% of the diversity variations (PC1) in bacterial community structures were affected mainly by incubation time with a higher

299 similarity between the communities in the initial time period (0, 7 and 14 days) than
300 those found later at 21, 28 and 50 days (Fig. 3A). The permutational multivariate
301 analysis of variance (PERMANOVA) of the data also indicates that the incubation time
302 caused the greatest effect on the bacterial community composition of the BPS
303 microcosm (PERMANOVA, $p = 0.001$), followed by the effect of the contamination
304 with the different PPCPs (PERMANOVA, $p < 0.005$). Similarly, analyses of the
305 bacterial communities by nonmetric multidimensional scaling (NMDS) also grouped the
306 samples according to incubation time (Fig. S1B). Therefore, the main deterministic
307 factor which affected the bacterial community composition of the BPSs was the
308 incubation time and, to a lesser extent, the treatment with PPCPs. Similar stronger
309 effects of aging of the BPS or incubation time has also been observed in other BPSs in
310 which the effects of pesticides application were studied (Marinozzi et al., 2013; Diez et
311 al., 2017; El Azhari et al 2018). When NMDS is constrained with data from the
312 bacterial phyla (Fig. 3B), *Bacteroidetes* contributed to the bacterial community
313 differentiation at 7 and 14 days, whereas *Actinobacteria*, *Acidobacteria, Chloroflexi,*
314 *Firmicutes* and *Planctomycetes* showed more influence at 14 and 21 days. Nevertheless,
315 the phyla *Gemmatimonadetes*, *Proteobacteria*, *Verrumicrobia* and *Saccharibacteria*
316 mainly influenced the bacteria community structure at 28 and 50 days. These tendencies
317 can also be observed in the relative abundance of these phyla in Fig. 2A in which
318 *Bacteroidetes* declined with time while, in contrast, *Planctomycetes*, *Acidobacteria* and
319 *Verrumicrobia* showed an opposite temporal trend, and *Actinobacteria* fluctuated with
320 time, showing maximum relative abundance at 21 and 28 days.

3.2.2.1 Impact of PPCPs on the composition of the bacterial communities

In order to determine the effects of the different PPCPs on the most abundant bacterial families (Fig. 4) as well as on bacterial taxa at the class/order levels (Fig. S2-S6), the relative abundances (RA) in the controls along time were compared with the RA in BPS submitted to the different PPCP treatments. In all BPS microcosms *Alphaproteobacteria* (19.9-40.1% RA) decreased during the first 14 days of incubation, but increased significantly in those exposed to IBP (ANOVA, $p < 0.05$) (Fig. 2A). The alphaproteobacterial orders *Rhodobacterales* and *Rickettsiales* were enriched in all cases along time, but were significantly reduced in those BPS treated with TCS or the mixture of PPCPs (Fig. S2). Within the order of *Rhodobacterales*, the dominant family *Hyphomonadaceae* (Fig. 4) was affected in a similar manner by IBP, TCS and by the PPCP mixture, indicating that this family is sensitive to these contaminants, but less so to DCF. The RA of the order *Caulobacterales,* (Fig. S2) was positively affected by IBP, and especially by TCS or the mix of PPCPs with a significant (ANOVA, $p < 0.05$) increase of 0.9-2% with respect to the control. The abundance of the family *Caulobacteraceae* (Fig. 4), increased by 1-2% at 14-28 days with TCS and the PPCPs mixture. Interestingly, microorganisms belonging to this family have been found to be involved in the degradation of other organic pollutants such as diclofop-methyl and phenanthrene (Zhang, H. et al., 2018; Lu, C. et al., 2019). In the current study, the observed enrichment within this family was mainly due to two OTUs (JN868839.1.1481 and FPLS01017875.18.1484) belonging to the genera *Brevundimonas* and *Caulobacter*, respectively, indicating that these caulobacterial genera may have some resistance to TCS. In the case of members of *Rhizobiales* (Fig. S2), exposure to IBP or TCS increased the RA compared to the control microcosms at 28 days and 7 days,

345 respectively. Nevertheless, DCF had a significant negative effect at 28 days (ANOVA,
346 $p < 0.05$). However, the dominant families of this order, *Hyphomicrobiaceae* and
347 *Rhizobiaceae* (Fig. 4), tend to increase in those BPS contaminated with the PPCP
348 mixture at the end of the incubation period when the concentrations had lowered
349 substantially. Exposure to IBP also significantly increased the RA of members of
350 *Sphingomonadales* at 14 days (Fig. S2), while for DCF, TCS and for the PPCPs
351 mixture, the RA decreased with respect to the control after 21 days, and especially after
352 28 days. In the same manner, treatment with IBP caused an increment in the family
353 *Sphingomonadaceae* whose RA increased between 1-2% at 7, 14 and 50 days (Fig. 4).
354 This increase is mainly associated to enrichment of the genus *Novosphingobium*.
355 Recently, Navrozidou et al. (2019) reported that *Novosphingobium* was a predominant
356 genus in activated sludge after application of a high dose of ibuprofen. Therefore, this
357 genus is likely to metabolize this PPCP. IBP-exposed microcosms were also enriched in
358 *Sphingobium* and *Sphingomonas* species at 7 and 50 days. Previous studies have
359 demonstrated that specialized microbiota belonging to these genera were capable of
360 degrading PPCPs (Zhou et al., 2013). In fact, Murdoch and Hay (2005) obtained an
361 isolate from activated sewage sludge, *Sphingomonas* sp. strain Ibu-2, with the ability to
362 use IBP as a sole carbon and energy source. This capacity is associated with a five-gene
363 cluster, *ipfABDEF*, which is involved in the transformation of ibuprofen to
364 isobutylcatechol, an alkylcatechol intermediate which bacteria may use for growth
365 (Murdoch and Hay, 2013). Similar genes have been observed in a strain belonging to
366 the alphaproteobacterial family *Rhodospirillaceae* (Żur et al., 2018), although generally
367 the RA of this family was reduced in IBP- exposed BPS (Fig. 4).

368 The relative abundance of *Betaproteobacteria* increased with time in all BPS
369 microcosms except in those treated with TCS. Within this class, microorganisms of the
370 order *Methylophilales* were mostly negatively impacted by TCS, showing a reduction in
371 the RA of 0.4-1% (Fig. S3A). However, the RA of *Burkholderiales* increased
372 significantly (ANOVA, $p < 0.05$) with respect to the control at several time periods with
373 IBP, DCF and the PPCPs mixture, but not when exposed to TCS. Interestingly, strains
374 belonging to this order have been found which harbour genes sharing similarity up to 76
375 % to known ibuprofen degradation genes (Żur et al., 2018), or with the capacity to
376 transform this compound (Murdoch and Hay, 2015).
377 On the other hand, the RA of *Gammaproteobacteria* decreased in the control BPS and
378 in those contaminated with TCS while it increased at punctual moments in the BPS
379 exposed to IBP, DCF or the PPCP mixture (Fig. 2A). In the case of the order
380 *Legionellales*, the relative abundance was 2.3 and 3.3 -fold lower in the BPSs exposed
381 to TCS at 28 and 50 days compared to controls, suggesting that members of this order
382 are sensitive even to low concentrations of this PPCP. However, DCF treatment caused
383 the opposite effect, pointing to tolerance to this contaminant (Fig. S3B). The
384 gammaproteobacterial order *Xanthomonadales* showed a decrease at 50 days in the
385 BPSs exposed to IBP when it was no longer present in the system but increased at
386 several time points with DCF and the PPCP mixture. Within this order, the family
387 *Xanthomonadaceae* was enriched at intermediate time points with IBP, DCF, TCS and
388 especially when the three contaminants were applied as a mixture (Fig. 4), suggesting
389 that members of this family are resistant or can metabolize these PPCPs. Interestingly,
390 species of this family have been determined as potential degraders of IBP, DCF, and
391 naproxen (Lu, Z. et al., 2019). Oh et al. (2019) also found enrichment of

392 *Xanthomonadaceae* in TCS -amended activated sludge reactors, specifically of the
393 genus *Pseudoxanothomonas.* Żur et al. (2018) reported that *Pseudoxanthomonas spadix*
394 BD-a59, a species with the ability to degrade all six BTEX (benzene, toluene,
395 ethylbenzene, and *o*-, *m*-, and *p*-xylene) compounds, has a gene cluster with a high
396 similarity with ibuprofen degradation genes *ipfABDEF*. Genera affected by PPCP -
397 treated BPSs included the xanthomonal genus *Luteimonas*, whose abundance increased
398 up to 2.5% especially with IBP and DCF (data not shown). Recently, Cydzik-
399 Kwiatkowska and Zielińska (2018) reported that this genus could play an important role
400 in the bioremoval of the emerging contaminant, bisphenol A. The abundance of another
401 dominant gammaproteobacterial family, *Pseudomonadaceae*, increased but not
402 significantly in the IBP -contaminated microcosms by 0.9% and 0.8% at 7 and 21 days,
403 respectively; and more substantially with the PPCP mixture at 14 days (Fig. 4),
404 especially with regard to the genus *Pseudomonas*.
405 Within the decrease of the RA of the phylum *Bacteroidetes* observed with time,
406 exposure to IBP and DCF induced a relatively stronger negative effect by decreasing
407 significantly (ANOVA, $p < 0.05$) by 3.8-15.6% and 8.3-11.3%, respectively (Fig. 2A).
408 Similarly, these contaminants negatively affected *Saprospirae*, one of the most
409 abundant classes of this phylum (Fig. S4). In contrast, the RA of the bacteroidetal class
410 *Sphingobacteriia* was higher after treatment with the PPCPs studied, especially in the
411 TCS contaminated BPS, and when applied as a mixture, showing a significant
412 (ANOVA, $p < 0.05$) increase in RA of 0.5-2.4% (Fig. S4). This enrichment was
413 reflected by the dominant family *Sphingobacteriaceae,* especially of the abundant OTU
414 AB267714.1.1482 belonging to the genus *Olivibacter*. Strains belonging to this genus
415 have been found to be involved in the degradation of phenanthrene (Villaverde et al.,

2019) or diphenol (Ntougias et al., 2014). On the other hand, treatment with TCS caused a decline in members of the class *Cytophagia* at 14 and 21 days by 3.4% and 3.9% respectively, but then increased by 6.5% at day 50 (Fig. S4), indicating a possible sensitivity of this class to TCS until concentrations decline to below the 10 mg kg^{-1} level. The most abundant bacteroidetal family in all BPSs was *Chitinophagaceae*, whose abundance decreased with time, especially in microcosms exposed to IBP and DCF (Fig. 4), although it was relatively unaffected in the TCS-exposed microcosms. PPCP application showed a significant (ANOVA, $p < 0.05$) increase in the abundance of the flavobacterial family *Cyclobacteriaceae* of which strains have been isolated from saline environments including oil-contaminated fields (Hu et al., 2015), but which have not been associated previously with PPCPs. A general decrease in *Bacteroidetes* was also observed in other studies with BPSs exposed to pesticides (Dealtry et al., 2016; Holmsgaard et al., 2017).

The RA of the phylum *Acidobacteria* increased over time in all BPS microcosms except in those contaminated with TCS individually or in mixture and in which its abundance was drastically reduced at 28 and 50 days of incubation (Fig. 2A). Within this phylum, the RA of the class *Acidobacteria-6* was 5 and 7- fold higher in control samples than in samples treated with TCS or the mix of PPCPs at 50 days, respectively (Fig. S5). Moreover, TCS treatment prevented the enrichment of the class *Chloracidobacteria*. This biocide negatively affected microorganisms of these two classes of *Acidobacteria*, especially the OTUs MEDJ01000003.85717.87273 and JN869200.1.1518 belonging to the families RB40 and Ellin6075, respectively.

The phyla *Verrumicrobia* showed enrichment during the incubation period. However, this increment was by 2- fold less pronounced in BPSs exposed to TCS, compared to

440 control conditions (Fig. 2A). The abundance of the class *Methylacidiphilae* was
441 significantly (ANOVA, $p < 0.05$) reduced by 0.9-1% after 21 or more days of exposure
442 to TCS or the mixture of PPCPs (Fig. S6A), mainly affecting the family LD19. In
443 contrast, the application of IBP caused enrichment of *Verrumicrobia* (Fig. 2A),
444 especially increasing the abundance of the class *Verrucomicrobiae* by between 0.6-1%
445 at 21 and 28 days. The same effect occurred after 21 days when all three PPCPs were
446 added in mixture (Fig. S6A). However, the dominant verrumicrobial family
447 *Verrucomicrobiaceae*, only showed substantial increases at the end of the incubation
448 period in those BPSs contaminated with IBP and the PPCP mixture (Fig 4).
449 The RA of the phylum *Planctomycetes* increased in all the BPS microcosms during the
450 incubation period (Fig. 2A). Recently, Zhang, S. et al. (2018) determined that
451 *Planctomycetes* together with *Proteobacteria* were the most abundant phyla in
452 biologically active filters exhibiting efficient removal of emerging contaminants. The
453 RA observed for the major planctomycetal class *Planctomycetia* showed trends similar
454 to the phylum on the whole (Fig. S6B). However, the most dominant family belonging
455 to this class, *Pirellulaceae*, showed enrichment at longer incubation times in BPSs
456 exposed to TCS or the PPCP mixture compared to the control BPS (Fig. 4). On the
457 other hand, the enrichment of the planctomycetal class *Phycisphaerae* observed in the
458 control was more pronounced in the BPSs exposed to IBP, but relatively less prominent
459 in samples treated with TCS or the PPCP mixture (Fig. S6B).
460 The RA of the phylum *Actinobacteria* showed an increasing trend in all the BPS
461 microcosms (Fig. 2A), although in the IBP and DCF treated BPSs there was a greater
462 increase at 14 days compared to the control BPS. Within this phylum, the RA of
463 *Promicromonosporaceae* generally increased in all PPCP treatments after 14 and 21

464 days of incubation (Fig. 4). These increments were mainly associated to the OTU
465 BBGM01000056.204.1722 belonging to the genus *Cellulosimicrobium*.
466 Finally, in order to verify the results of the community analysis based on 16S rRNA
467 sequences, the abundance of some of the taxa most affected by contamination with
468 PPCPs (*Alpha-, Beta-, Gammaproteobacteria* and *Acidobacteria*) was quantified by
469 real-time PCR assays (Table S1). As expected, no significant difference in the
470 abundance of *Alpha-,* and *Gammaproteobacteria* at the class level was observed in any
471 microcosms between the initial (7 days) and final (50 days) time points. Nevertheless,
472 the bacteria belonging to the *Betaproteobacteria* class were enriched in BPS
473 microcosms after contamination with IBP or DCF but not the BPSs exposed to TCS or
474 the PPCP mixture. Moreover, in accordance with the 16S rRNA community study
475 results, the abundance of the phylum *Acidobacteria* increased in control samples and in
476 the microcosms treated with IBP and DCF, but no significant differences were observed
477 in the TCS-exposed microcosms. Therefore, the results obtained by qPCR analysis were
478 consistent with 16S rRNA gene sequencing data.
479 *3.3. Toxicological study*
480 In order to discern whether the PPCPs at the concentrations used in this study have a
481 lethal effect on the total bacterial populations in the BPS microcosms, the number of
482 live bacterial cells was determined by the LIVE/DEAD® microscopic technique (Fig.
483 5). Before contamination, the number of live bacterial cells in the BPS was $1.03 \times 10^9 \pm$
484 5.48×10^7 cells/g. Throughout the incubation period, the number of cells in the BPSs
485 treated with IBP or DCF was not significantly different than in the non-contaminated
486 BPS microcosm (Control). However, after 7 and 14 days, the BPS exposed to TCS
487 contained 43% and 34% less live bacterial cells, respectively, than the control BPS

(ANOVA, $p > 0.01$) before recovering at later periods. This may be due to the fact that the TCS exposed BPS still contained more than 65% of the initially applied biocide at these times. Nevertheless, when the three PPCPs were applied in mixture, the observed decrease in viability during the same period was not significant. These results suggest that the bactericidal effect of TCS is related to its concentration in the BPS although the bacterial community recovered with time. On the other hand, the lethal effect of TCS was mitigated in BPS contaminated with the three PPCPs, possibly due to the increase of resistant populations induced by IBP and/or DCF. Further studies with different concentrations will be needed to determine toxicity limits of the PPCPs in BPS.

4. Conclusions

The BPS system is effective in dissipating PPCPs, especially IBP followed by DCF. However, dissipation of DCF is slowed down when the PPCPs are applied as a mixture. This may be due to the negative impact of TCS on some of the bacterial groups. The PPCPs affect the bacterial community although the incubation time is the major driver. Of the three PPCPs, TCS had the most negative impact on bacterial viability and the community, probably due to its antiseptic effect even at relatively low concentrations. Nevertheless, the relative abundance of certain bacterial taxa increased with all the PPCPs. Our results suggest that BPSs after the treatments with IBP, DCF and TCS can maintain high bacterial community diversity despite the contamination levels and biocide agents added. It would be interesting in future works to determine which mechanisms are used by members of the most resistant taxa to detoxify these PPCPs. Altogether, the ecotoxicity and effect on bacterial communities by the PPCPs studied, especially TCS, should be taken into account not only for techniques which could be

used to eliminate PPCPs from effluents but also for the ecological effects of low concentrations in the environment.

CRediT authorship contribution statement

Inés Aguilar-Romero: Investigation; Data curation, Formal analysis, Visualization, Writing - original draft. Esperanza Romero: Funding acquisition, Supervision, Writing - review & editing. Regina-Michaela Wittich: Conceptualization, Writing - review & editing. Pieter van Dillewijn: Funding acquisition, Conceptualization, Supervision, Writing - review & editing.

Declaration of competing interest

The authors declare that they have no known competing financial interests or personal relationships that could have appeared to influence the work reported in this paper.

Acknowledgements

This study was supported by the Spanish Ministerio de Economía y Competitividad and the Agencia Estatal de Investigación (AEI) (projects CTM2013-44271-R and CTM2017-86504-R), and co-financing from the European Regional Development Fund (ERDF). Inés Aguilar-Romero thanks her FPI grant.

Appendix A. Supplementary data

Related supplementary material.

References

Aguilar-Romero, I., van Dillewijn, P., Nesme, J., Sorensen, S.J., Romero, E., 2019. Improvement of pesticide removal in contaminated media using aqueous extracts from contaminated biopurification systems. Sci. Total Environ. 691, 749-759. doi: 10.1016/j.scitotenv.2019.07.087.

Aranami, K., Readman, J.W., 2007. Photolytic degradation of triclosan in freshwater and seawater. Chemosphere 66, 1052-1056. doi: 10.1016/j.chemosphere.2006.07.010.

Caporaso, J.G., Bittinger, K., Bushman, F.D., DeSantis, T.Z., Andersen, G.L., Knight, R., 2010a. PyNAST: a flexible tool for aligning sequences to a template alignment. Bioinformatics 26, 266-7. doi: 10.1093/bioinformatics/btp636.

Caporaso, J.G., Kuczynski, J., Stombaugh, J., Bittinger, K., Bushman, F.D., Costello, E.K., Fierer, N., Pena, A.G., Goodrich, J.K., Gordon, J.I., Huttley, G.A., Kelley, S.T., Knights, D., Koenig, J.E., Ley, R.E., Lozupone, C.A., McDonald, D., Muegge, B.D., Pirrung, M., Reeder, J., Sevinsky, J.R., Turnbaugh, P.J., Walters, W.A., Widmann, J., Yatsunenko, T., Zaneveld, J., Knight, R., 2010b. QIIME allows analysis of high-throughput community sequencing data. Nat. Methods 7, 335-6. doi: 10.1038/nmeth.f.303.

Castiglioni, S., Bagnati, R., Calamari, D., Fanelli, R., Zuccato, E., 2005. A multiresidue analytical method using solid-phase extraction and high-pressure liquid chromatography tandem mass spectrometry to measure pharmaceuticals of different therapeutic classes in urban wastewaters. J. Chromatogr. A 1092, 206-215. doi: 10.1016/j.chroma.2005.07.012.

Castillo Diaz, J.M., Delgado-Moreno, L., Nunez, R., Nogales, R., Romero, E., 2016. Enhancing pesticide degradation using indigenous microorganisms isolated under high pesticide load in bioremediation systems with vermicomposts. Bioresour. Technol. 214, 234-41. doi: 10.1016/j.biortech.2016.04.105.

Castillo, M.D.P., Torstensson, L., Stenström, J., 2008. Biobeds for environmental protection from pesticide use - A review. J. Agric. Food Chem. 56, 6206-6219. doi: 10.1021/jf800844x.

Castro-Gutiérrez, V., Masís-Mora, M., Diez, M.C., Tortella, G.R., Rodríguez-Rodríguez, C.E., 2017. Aging of biomixtures: Effects on carbofuran removal and microbial community structure. Chemosphere 168, 418-425. 10.1016/j.chemosphere.2016.10.065.

Clarke, A., Azulai, D., Elias Dueker, M., Vos, M., Perron, G.G., 2019. Triclosan alters microbial communities in freshwater microcosms. Water 11. doi: 10.3390/w11050961.

Comeau, A.M., Douglas, G.M., Langille, M.G., 2017. Microbiome helper: a custom and streamlined workflow for microbiome research. mSystems 2. doi: 10.1128/mSystems.00127-16.

Cydzik-Kwiatkowska, A., Zielińska, M., 2018. Microbial composition of biofilm treating wastewater rich in bisphenol A. J. Environ. Sci. Health, Part A 53, 385-392. doi: 10.1080/10934529.2017.1404326.

Daughton, C.G., Ternes, T.A., 1999. Pharmaceuticals and personal care products in the environment: Agents of subtle change? Environ. Health Perspect. 107, 907-938. doi: 10.1289/ehp.99107s6907.

581 Dealtry, S., Nour, E.H., Holmsgaard, P.N., Ding, G.C., Weichelt, V., Dunon, V., Heuer,
582 H., Hansen, L.H., Sørensen, S.J., Springael, D., Smalla, K., 2016. Exploring the
583 complex response to linuron of bacterial communities from biopurification
584 systems by means of cultivation-independent methods. FEMS Microbiol. Ecol.
585 92. doi: 10.1093/femsec/fiv157.
586 De Wilde, T., Spanoghe, P., Debaer, C., Ryckeboer, J., Springael, D., Jaeken, P., 2007.
587 Overview of on-farm bioremediation systems to reduce the occurrence of point
588 source contamination. Pest Manage. Sci. 63, 111-128. doi: 10.1002/ps.1323.
589 Delgado-Moreno, L., Bazhari, S., Nogales, R., Romero, E., 2019. Innovative application
590 of biobed bioremediation systems to remove emerging contaminants: Adsorption,
591 degradation and bioaccesibility. Sci. Total Environ. 651, 990-997. doi:
592 https://doi.org/10.1016/j.scitotenv.2018.09.268.
593 Dias, L.D.A., Gebler, L., Niemeyer, J.C., Itako, A.T., 2020. Destination of pesticide
594 residues on biobeds: State of the art and future perspectives in Latin America.
595 Chemosphere 248. doi: 10.1016/j.chemosphere.2020.126038.
596 Diez, M.C., Elgueta, S., Rubilar, O., Tortella, G.R., Schalchli, H., Bornhardt, C.,
597 Gallardo, F., 2017. Pesticide dissipation and microbial community changes in a
598 biopurification system: influence of the rhizosphere. Biodegradation 28, 395-412.
599 doi: 10.1007/s10532-017-9804-y.
600 Diez, M.C., Leiva, B., Gallardo, F., 2018. Novel insights in biopurification system for
601 dissipation of a pesticide mixture in repeated applications. Environmental Sci.
602 Pollut. Res. 25, 21440-21450. doi: 10.1007/s11356-017-0130-z.

603 Ebele, A.J., Abou-Elwafa Abdallah, M., Harrad, S., 2017. Pharmaceuticals and personal
604 care products (PPCPs) in the freshwater aquatic environment. Emerg. Contam. 3,
605 1-16. doi: 10.1016/j.emcon.2016.12.004.
606 Edgar, R.C., Haas, B.J., Clemente, J.C., Quince, C., Knight, R., 2011. UCHIME
607 improves sensitivity and speed of chimera detection. Bioinformatics 27, 2194-
608 200. doi: 10.1093/bioinformatics/btr381.
609 El Azhari, N., Dermou, E., Barnard, R.L., Storck, V., Tourna, M., Beguet, J., Karas,
610 P.A., Lucini, L., Rouard, N., Botteri, L., Ferrari, F., Trevisan, M., Karpouzas,
611 D.G., Martin-Laurent, F., 2018. The dissipation and microbial ecotoxicity of
612 tebuconazole and its transformation products in soil under standard laboratory and
613 simulated winter conditions. Sci Total Environ 637-638, 892-906. doi:
614 10.1016/j.scitotenv.2018.05.088.
615 Gee, R.H., Charles, A., Taylor, N., Darbre, P.D., 2008. Oestrogenic and androgenic
616 activity of triclosan in breast cancer cells. J. Appl. Toxicol. 28, 78-91. doi:
617 10.1002/jat.1316.
618 Geens, T., Neels, H., Covaci, A., 2012. Distribution of bisphenol-A, triclosan and n-
619 nonylphenol in human adipose tissue, liver and brain. Chemosphere 87, 796-802.
620 doi: 10.1016/j.chemosphere.2012.01.002.
621 Góngora-Echeverría, V.R., Quintal-Franco, C., Arena-Ortiz, M.L., Giácoman-Vallejos,
622 G., Ponce-Caballero, C., 2018. Identification of microbial species present in a
623 pesticide dissipation process in biobed systems using typical substrates from
624 southeastern Mexico as a biomixture at a laboratory scale. Sci. Total Environ.
625 628-629, 528-538. doi:10.1016/j.scitotenv.2018.02.082.

626 Grassi, M., Rizzo, L., Farina, A., 2013. Endocrine disruptors compounds,
627 pharmaceuticals and personal care products in urban wastewater: Implications for
628 agricultural reuse and their removal by adsorption process. Environ. Sci. Pollut.
629 Res. 20, 3616-3628. doi: 10.1007/s11356-013-1636-7.
630 Holmsgaard, P.N., Dealtry, S., Dunon, V., Heuer, H., Hansen, L.H., Springael, D.,
631 Smalla, K., Riber, L., Sørensen, S.J., 2017. Response of the bacterial community
632 in an on-farm biopurification system to which diverse pesticides are introduced
633 over an agricultural season. Environ. Pollut. 229, 854-862. Doi:
634 10.1016/j.envpol.2017.07.026.
635 Houtman, C.J., 2010. Emerging contaminants in surface waters and their relevance for
636 the production of drinking water in Europe. J. Integr. Environ. Sci. doi:
637 10.1080/1943815x.2010.511648.
638 Hu, B., Yang, Q., Cai, M., Tang, Y.-Q., Zhao, G.-F., Wu, X.-L., 2015. *Negadavirga*
639 *shengliensis* gen. nov., sp. nov., a novel member of the family *Cyclobacteriaceae*
640 isolated from oil-contaminated saline soil. Antonie van Leeuwenhoek 107, 663-
641 673. doi: 10.1007/s10482-014-0361-7.
642 Jiang, C., Geng, J., Hu, H., Ma, H., Gao, X., Ren, H., 2017. Impact of selected non-
643 steroidal anti-inflammatory pharmaceuticals on microbial community assembly
644 and activity in sequencing batch reactors. PLoS One 12, e0179236. doi:
645 10.1371/journal.pone.0179236.
646 Jung, E.M., An, B.S., Choi, K.C., Jeung, E.B., 2012. Potential estrogenic activity of
647 triclosan in the uterus of immature rats and rat pituitary GH3 cells. Toxicol. Lett.
648 208, 142-148. doi: 10.1016/j.toxlet.2011.10.017.

649 Karas, P.A., Perruchon, C., Karanasios, E., Papadopoulou, E.S., Manthou, E., Sitra, S.,
650 Ehaliotis, C., Karpouzas, D.G., 2016. Integrated biodepuration of pesticide-
651 contaminated wastewaters from the fruit-packaging industry using biobeds:
652 Bioaugmentation, risk assessment and optimized management. J. Hazard. Mater.
653 320, 635-644. doi: 10.1016/j.jhazmat.2016.07.071.
654 Lonappan, L., Brar, S.K., Das, R.K., Verma, M., Surampalli, R.Y., 2016. Diclofenac
655 and its transformation products: Environmental occurrence and toxicity - A
656 review. Environ. Int. 96, 127-138. doi: 10.1016/j.envint.2016.09.014.
657 Lu, C., Hong, Y., Liu, J., Gao, Y., Ma, Z., Yang, B., Ling, W., Waigi, M.G., 2019. A
658 PAH-degrading bacterial community enriched with contaminated agricultural soil
659 and its utility for microbial bioremediation. Environ. Pollut. 251, 773-782. doi:
660 10.1016/j.envpol.2019.05.044.
661 Lu, Z., Sun, W., Li, C., Ao, X., Yang, C., Li, S., 2019. Bioremoval of non-steroidal anti-
662 inflammatory drugs by *Pseudoxanthomonas* sp. DIN-3 isolated from biological
663 activated carbon process. Wat. Res. 161, 459-472. doi:
664 10.1016/j.watres.2019.05.065.
665 Maldonado-Torres, S., Gurung, R., Rijal, H., Chan, A., Acharya, S., Rogelj, S.,
666 Piyasena, M., Rubasinghege, G., 2018. Fate, transformation, and toxicological
667 impacts of pharmaceutical and personal care products in surface waters. Environ.
668 Health Ins. 12. doi: 10.1177/1178630218795836.
669 Marinozzi, M., Coppola, L., Monaci, E., Karpouzas, D.G., Papadopoulou, E.,
670 Menkissoglu-Spiroudi, U., Vischetti, C., 2013. The dissipation of three fungicides
671 in a biobed organic substrate and their impact on the structure and activity of the

672 microbial community. Environ. Sci. Pollut. Res. 20, 2546-2555. doi:
673 10.1007/s11356-012-1165-9.
674 Murdoch, R.W., Hay, A.G., 2005. Formation of catechols via removal of acid side
675 chains from ibuprofen and related aromatic acids. Appl. Environ. Microbiol. 71,
676 6121-5. doi: 10.1128/AEM.71.10.6121-6125.2005.
677 Murdoch, R.W., Hay, A.G., 2013. Genetic and chemical characterization of ibuprofen
678 degradation by *Sphingomonas* Ibu-2. Microbiology 159, 621-32. doi:
679 10.1099/mic.0.062273-0.
680 Murdoch, R.W., Hay, A.G., 2015. The biotransformation of ibuprofen to
681 trihydroxyibuprofen in activated sludge and by *Variovorax* Ibu-1. Biodegradation
682 26, 105-13. doi: 10.1007/s10532-015-9719-4.
683 Navrozidou, E., Melidis, P., Ntougias, S., 2019. Biodegradation aspects of ibuprofen
684 and identification of ibuprofen-degrading microbiota in an immobilized cell
685 bioreactor. Environ. Sci. Pollut. Res. doi: 10.1007/s11356-019-04771-5.
686 Ntougias, S., Lapidus, A., Han, J., Mavromatis, K., Pati, A., Chen, A., Klenk, H.P.,
687 Woyke, T., Fasseas, C., Kyrpides, N.C., Zervakis, G.I., 2014. High quality draft
688 genome sequence of *Olivibacter* sitiensis type strain (AW-6^T), a diphenol
689 degrader with genes involved in the catechol pathway. Stand Genomic Sci 9, 783-
690 93. doi: 10.4056/sigs.5088950.
691 Oh, S., Choi, D., Cha, C.J., 2019. Ecological processes underpinning microbial
692 community structure during exposure to subinhibitory level of triclosan. Sci. Rep.
693 9. doi: 10.1038/s41598-019-40936-5.

694 Olaniyan, L.W.B., Mkwetshana, N., Okoh, A.I., 2016. Triclosan in water, implications
695 for human and environmental health. SpringerPlus 5. doi: 10.1186/s40064-016-
696 3287-x.
697 Peng, F.J., Diepens, N.J., Pan, C.G., Ying, G.G., Salvito, D., Selck, H., Van den Brink,
698 P.J., 2019. Response of sediment bacterial community to triclosan in subtropical
699 freshwater benthic microcosms. Environ. Pollut., 676-683. doi:
700 10.1016/j.envpol.2019.02.061.
701 Petrović, M., Gonzalez, S., Barceló, D., 2003. Analysis and removal of emerging
702 contaminants in wastewater and drinking water. Trends Anal. Chem. 22, 685-696.
703 doi: 10.1016/S0165-9936(03)01105-1.
704 Philippot, L., Tscherko, D., Bru, D., Kandeler, E., 2011. Distribution of high bacterial
705 taxa across the chronosequence of two alpine glacier forelands. Microb. Ecol. doi:
706 10.1007/s00248-010-9754-y.
707 Quast, C., Pruesse, E., Yilmaz, P., Gerken, J., Schweer, T., Yarza, P., Peplies, J.,
708 Glockner, F.O., 2013. The SILVA ribosomal RNA gene database project:
709 improved data processing and web-based tools. Nucleic Acids Res. 41, D590-6.
710 doi: 10.1093/nar/gks1219.
711 Rosal, R., Rodríguez, A., Perdigón-Melón, J.A., Petre, A., García-Calvo, E., Gómez,
712 M.J., Agüera, A., Fernández-Alba, A.R., 2010. Occurrence of emerging pollutants
713 in urban wastewater and their removal through biological treatment followed by
714 ozonation. Wat. Res. 44, 578-588. doi: 10.1016/j.watres.2009.07.004.
715 Tortella, G.R., Mella-Herrera, R.A., Sousa, D.Z., Rubilar, O., Acuña, J.J., Briceño, G.,
716 Diez, M.C., 2013. Atrazine dissipation and its impact on the microbial
717 communities and community level physiological profiles in a microcosm

718 simulating the biomixture of on-farm biopurification system. J. Hazard. Mat. 260,
719 459-467. doi: 10.1016/j.jhazmat.2013.05.059.
720 Villaverde, J., Láiz, L., Lara-Moreno, A., González-Pimentel, J.L., Morillo, E., 2019.
721 Bioaugmentation of PAH-contaminated soils with novel specific degrader strains
722 isolated from a contaminated industrial site. Effect of hydroxypropyl-β-
723 cyclodextrin as PAH bioavailability enhancer. Front. Microbiol. 10. doi:
724 10.3389/fmicb.2019.02588.
725 Walters, W., Hyde, E.R., Berg-Lyons, D., Ackermann, G., Humphrey, G., Parada, A.,
726 Gilbert, J.A., Jansson, J.K., Caporaso, J.G., Fuhrman, J.A., Apprill, A., Knight,
727 R., 2016. Improved bacterial 16S rRNA gene (V4 and V4-5) and fungal internal
728 transcribed spacer marker gene primers for microbial community surveys.
729 mSystems 1. doi: 10.1128/mSystems.00009-15.
730 Wilkinson, J., Hooda, P.S., Barker, J., Barton, S., Swinden, J., 2017. Occurrence, fate
731 and transformation of emerging contaminants in water: An overarching review of
732 the field. Environ. Pollut. 231, 954-970. doi: 10.1016/j.envpol.2017.08.032.
733 Zhang, H., Yu, T., Li, J., Wang, Y.R., Wang, G.L., Li, F., Liu, Y., Xiong, M.H., Ma,
734 Y.Q., 2018. Two *dcm* gene clusters essential for the degradation of diclofop-
735 methyl in a microbial consortium of *Rhodococcus* sp. JT-3 and *Brevundimonas*
736 sp. JT-9. J. Agr. Food Chem. 66, 12217-12226.. doi: 10.1021/acs.jafc.8b05382.
737 Zhang, S., Courtois, S., Gitungo, S., Raczko, R.F., Dyksen, J.E., Li, M., Axe, L., 2018.
738 Microbial community analysis in biologically active filters exhibiting efficient
739 removal of emerging contaminants and impact of operational conditions. Sci.
740 Total Environ. 640-641, 1455-1464. doi: 10.1016/j.scitotenv.2018.06.027.

741 Zhou, N.A., Lutovsky, A.C., Andaker, G.L., Gough, H.L., Ferguson, J.F., 2013.
742 Cultivation and characterization of bacterial isolates capable of degrading
743 pharmaceutical and personal care products for improved removal in activated
744 sludge wastewater treatment. Biodegradation 24, 813-827.
745 Żur, J., Piński, A., Marchlewicz, A., Hupert-Kocurek, K., Wojcieszyńska, D., Guzik,
746 U., 2018. Organic micropollutants paracetamol and ibuprofen-toxicity,
747 biodegradation, and genetic background of their utilization by bacteria. Environ.
748 Sci. Pollut. Res. 25, 21498-21524. doi: 10.1007/s11356-018-2517-x.
749

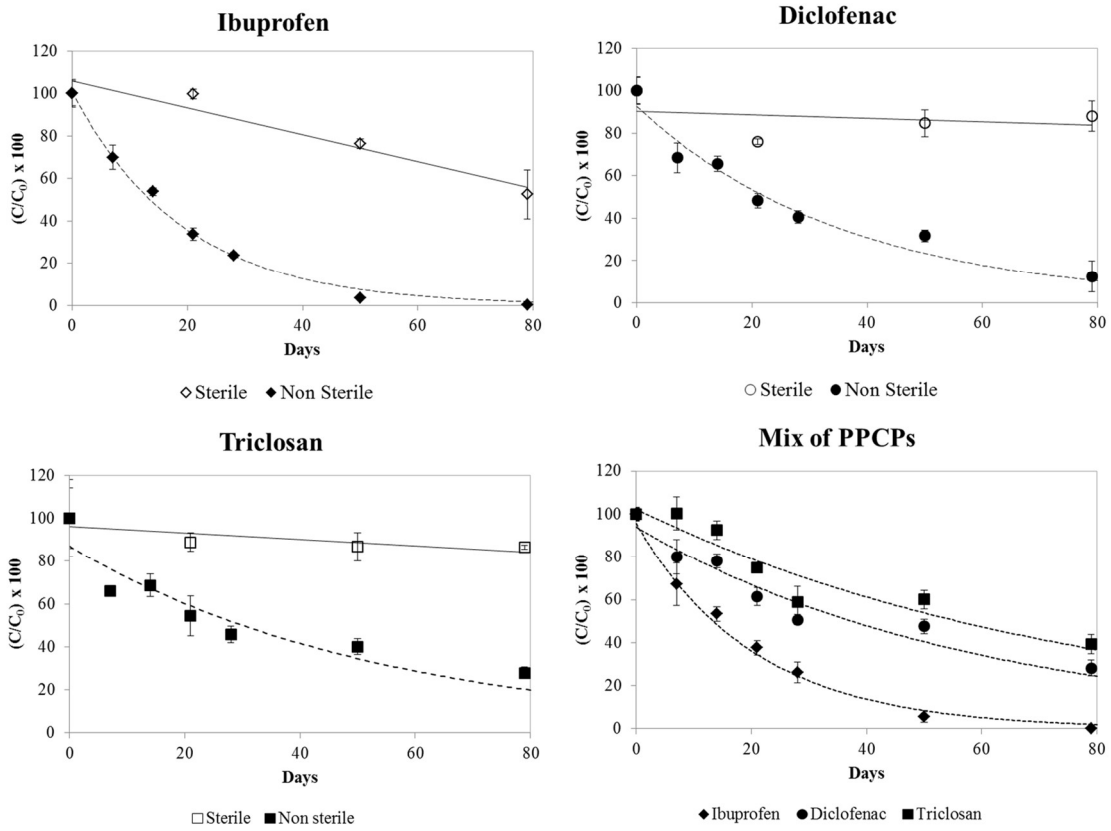

Figure 1. Dissipation of ibuprofen, diclofenac and triclosan applied separately or in mixture in non-sterilized (black symbols) and sterilized (white symbols) BPS microcosms. Lines represent the model fit to experimental data. Error bars indicate standard deviation (n=3).

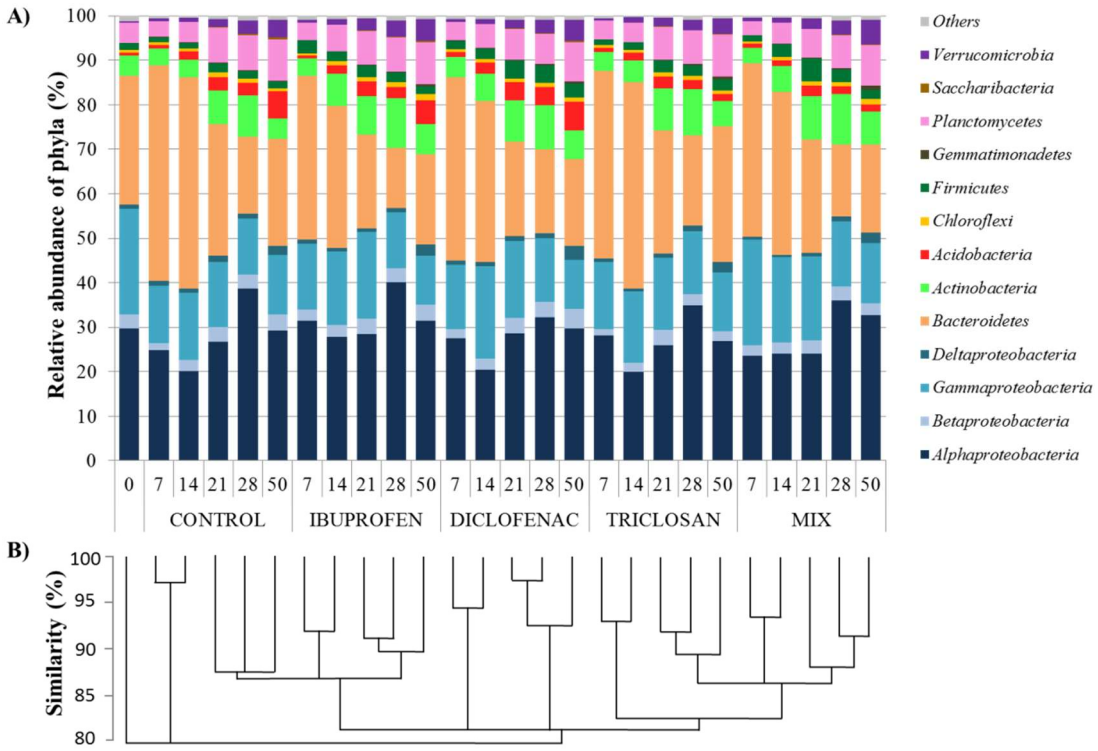

759

760

761 Figure 2. Relative abundance of the most dominant phyla (>1% in any sample) and
762 classes of *Proteobacteria* at different incubation times (days) in non-contaminated
763 (control) and contaminated BPS microcosms with ibuprofen, diclofenac and triclosan,
764 applied separately or in mixture (A). Hierarchical cluster analysis of the bacterial
765 community composition based on Bray-Curtis distances (B).

766

767

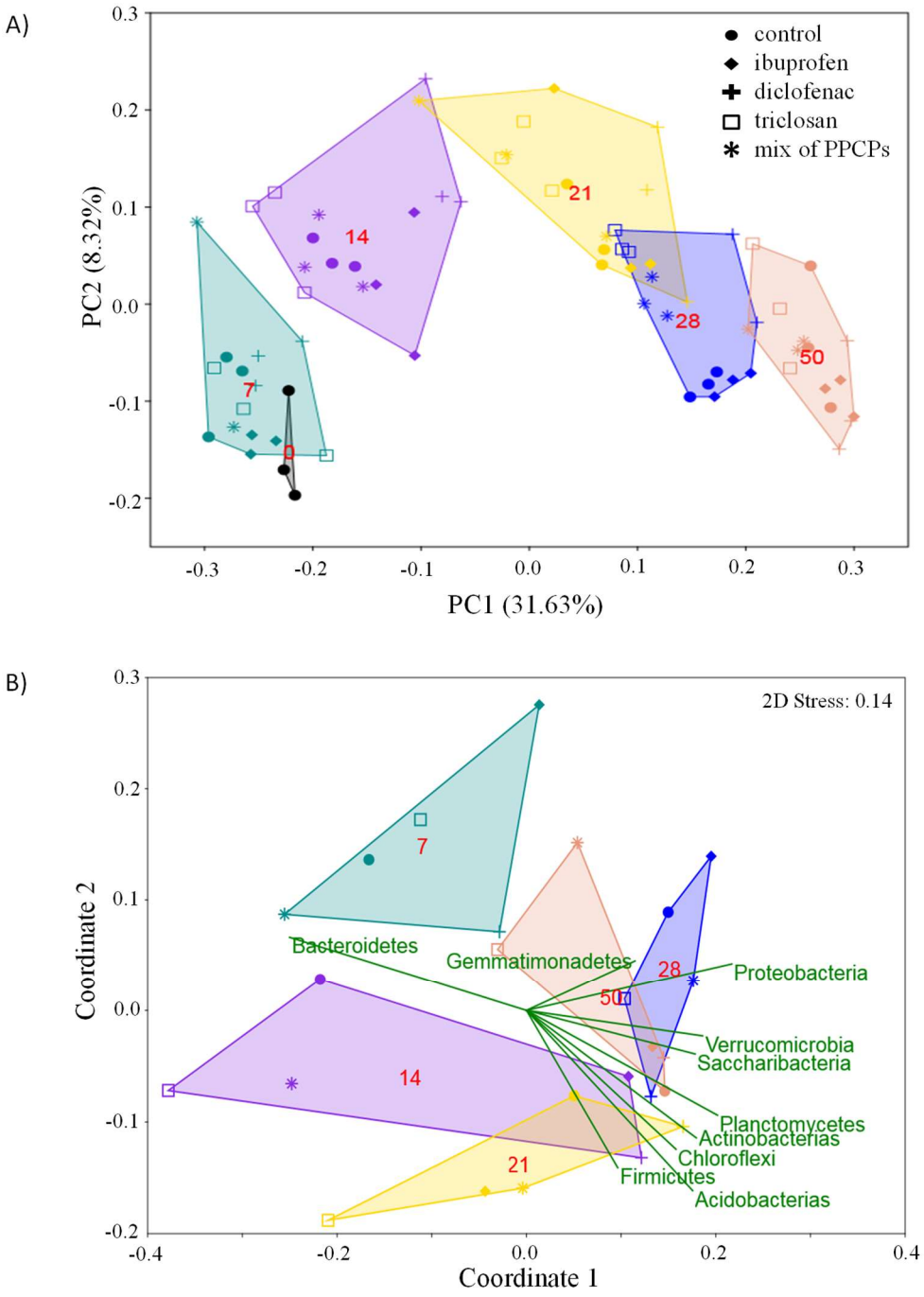

768

769 Figure 3. Principal coordinates analysis of bacterial communities in the BPS
770 microcosms based on Bray-Curtis distances (A). Nonmetric Multidimensional Scaling
771 (NMDS) ordination of the bacterial community composition based on Bray-Curtis
772 distances with data constrained to the most dominant phyla (B). The numbers in red
773 indicate the incubation time (days).

774 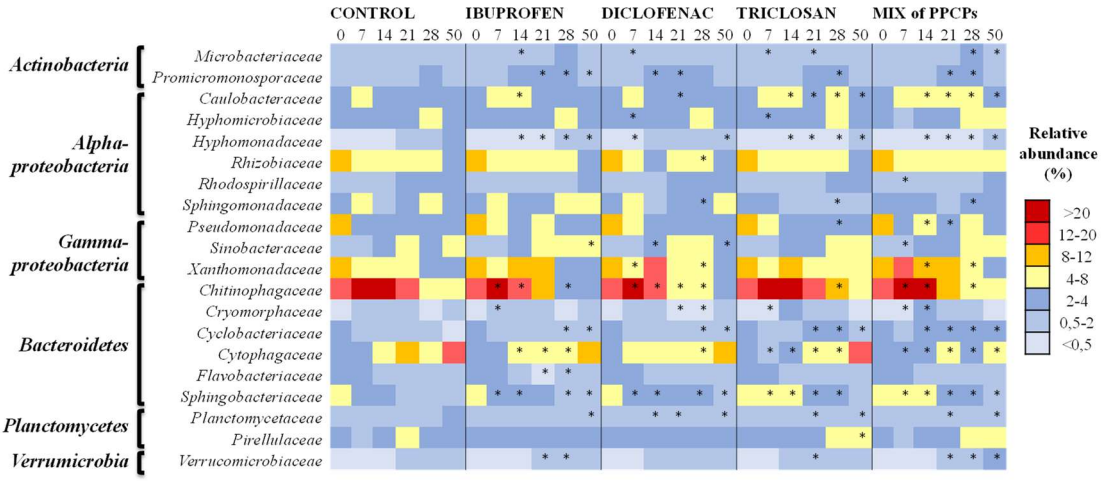

775

776 Figure 4. Heatmap of the most dominant families (>2% in any sample) in non-
777 contaminated (control) and BPS microcosms contaminated with ibuprofen, diclofenac
778 and triclosan, applied separately or in mixture at different incubation times (days).
779 *Significant differences among non-contaminated and contaminated BPS samples
780 (ANOVA homogeneity test; $p < 0.05$).

781

782

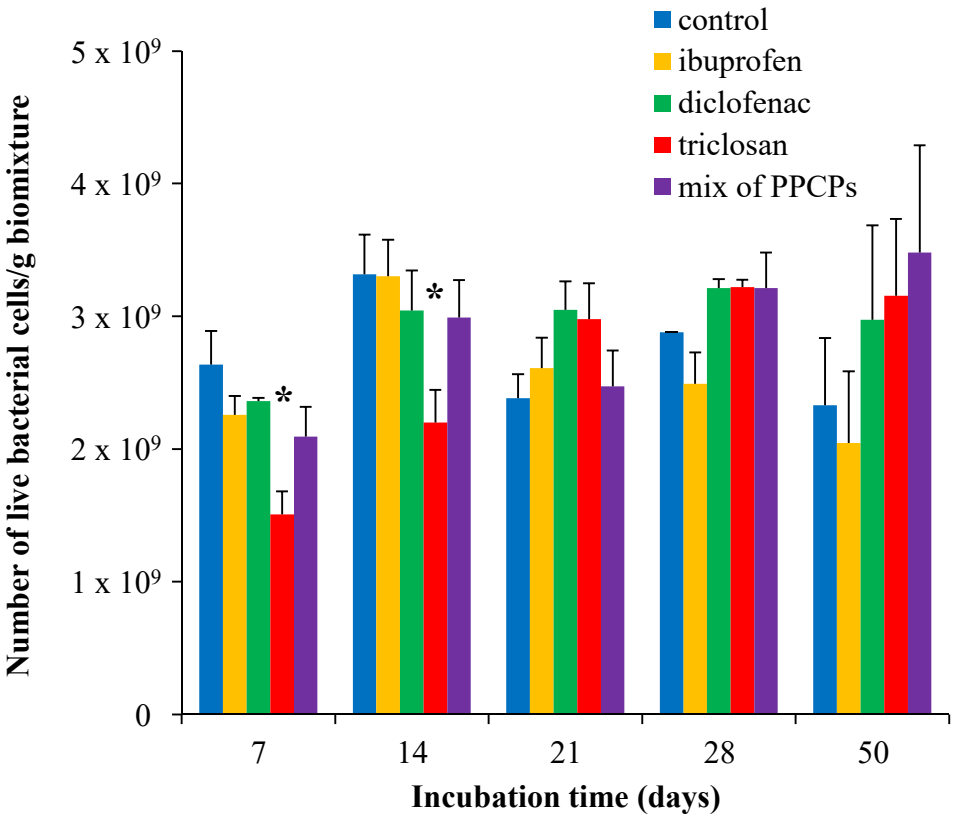

783

784

785 Figure 5. Number of live bacterial cells determined using the LIVE/DEAD®
786 BacLight™ Bacterial Viability Kit per gram of non-contaminated (control) and BPS
787 microcosm contaminated with ibuprofen, diclofenac and triclosan, applied separately or
788 in mixture at different incubation times. The number of live bacterial cells in the BPS
789 was initially 1.03 x 10^9 ± 5.48 x 10^7 cells/g. *Significant differences among non-
790 contaminated and contaminated BPS samples (ANOVA homogeneity test; $p < 0.01$).
791 Error bars represent the standard error for each sample (n>2).

792

793

Supplementary Data

Bacterial ecotoxicity and shifts in bacterial communities associated with the removal of ibuprofen, diclofenac and triclosan in biopurification systems

Inés Aguilar-Romero, Esperanza Romero, Regina-Michaela Wittich, and Pieter van Dillewijn*

Departamento de Protección Ambiental. Estación Experimental del Zaidín - Consejo Superior de Investigaciones Científicas (EEZ-CSIC). Calle Profesor Albareda 1, 18008 Granada. Spain.

.

* Corresponding author, e-mail: pieter.vandillewijn@eez.csic.es

809

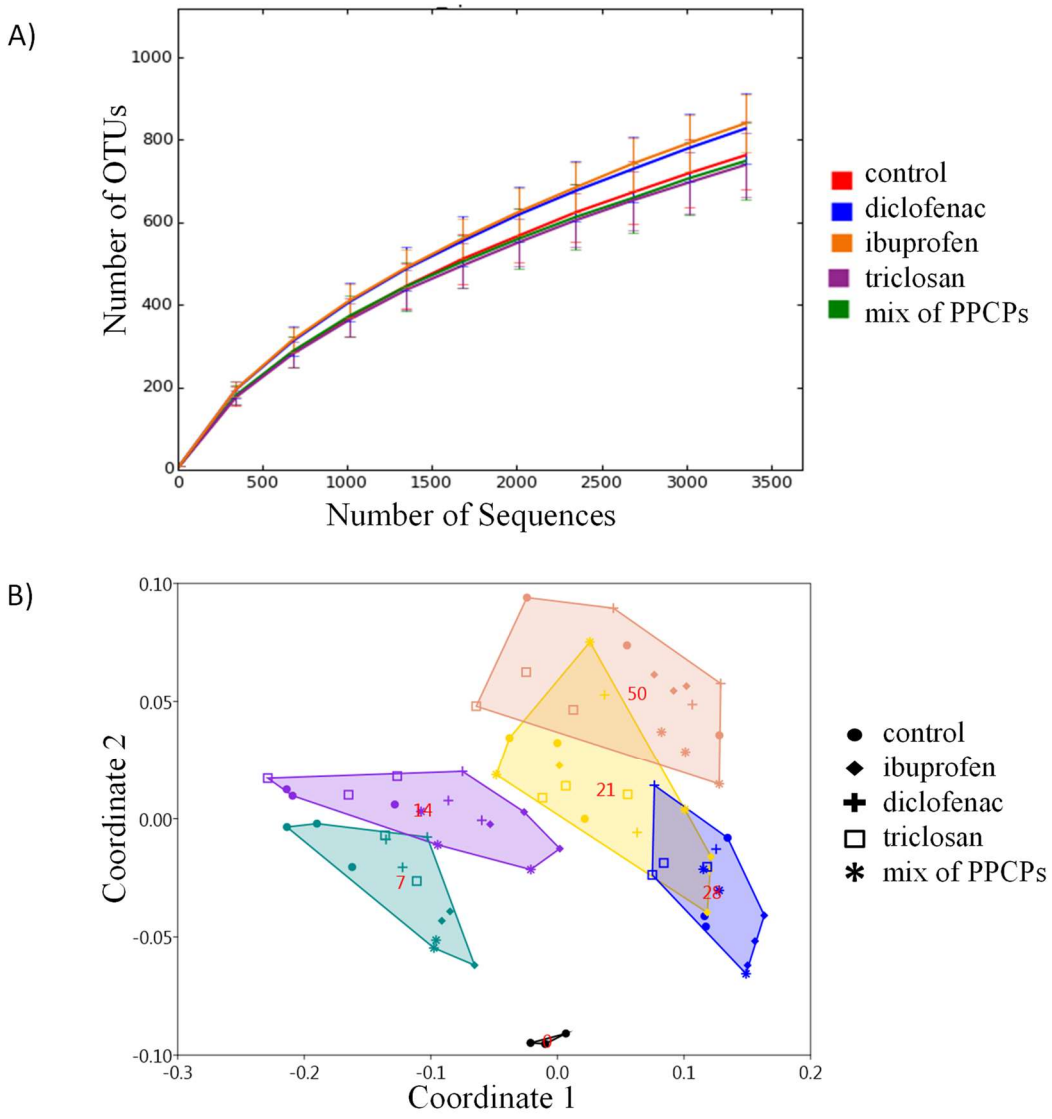

810

811 Figure S1. Rarefaction curves for the Operational Taxonomic Units (OTUs) of the non-
812 contaminated (control) and contaminated BPS samples with ibuprofen, diclofenac and
813 triclosan, applied separately and in mixture (A). Nonmetric Multidimensional Scaling
814 (NMDS) ordination of the bacterial community composition based on Bray-Curtis
815 distances. The numbers in red indicate the incubation time (days) (B).

816

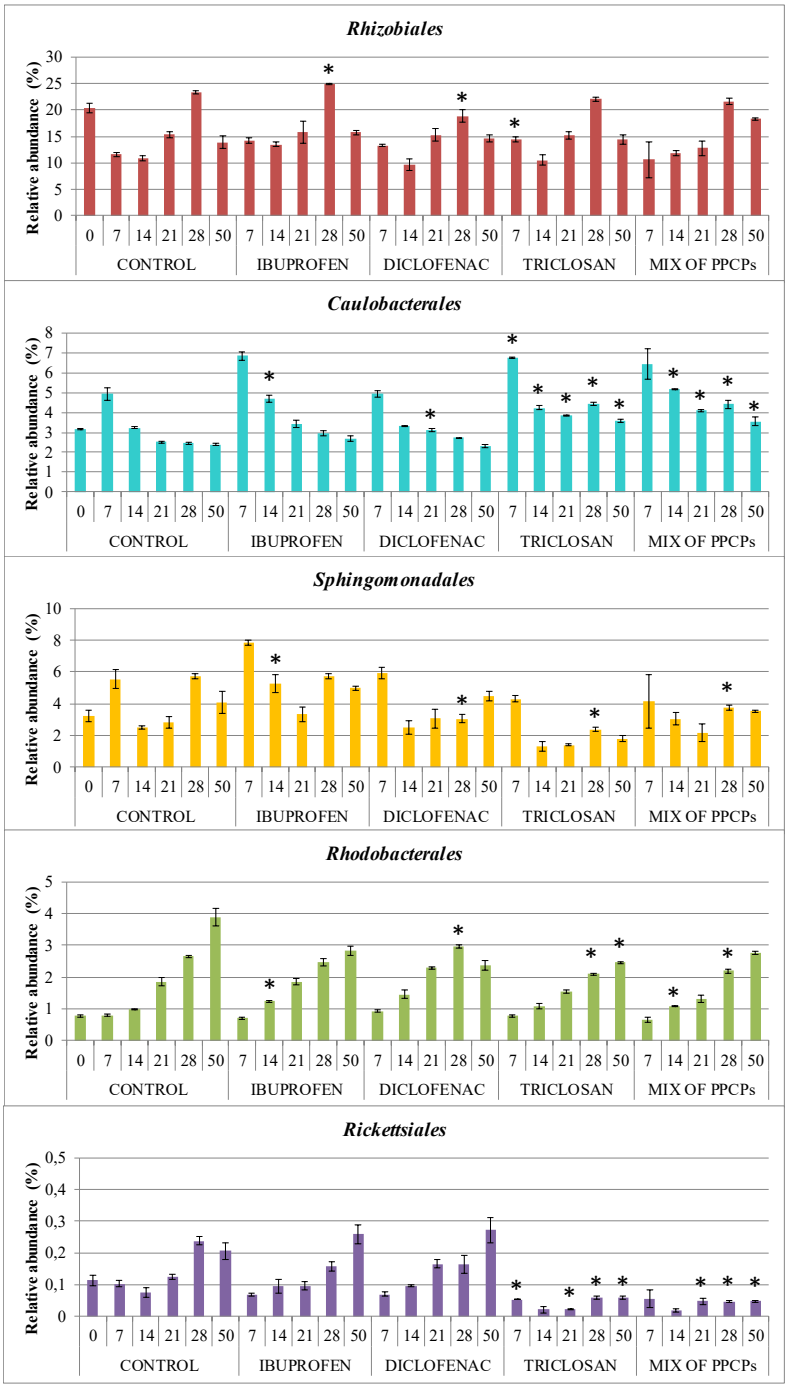

Figure S2. Relative abundance of different orders within the class *Alphaproteobacteria*. *Significant differences among non-contaminated (control) and contaminated BPS samples with ibuprofen, diclofenac and triclosan, applied separately and in mixture (ANOVA homogeneity test; $p < 0.05$). Error bars represent the standard error for each sample (n=3).

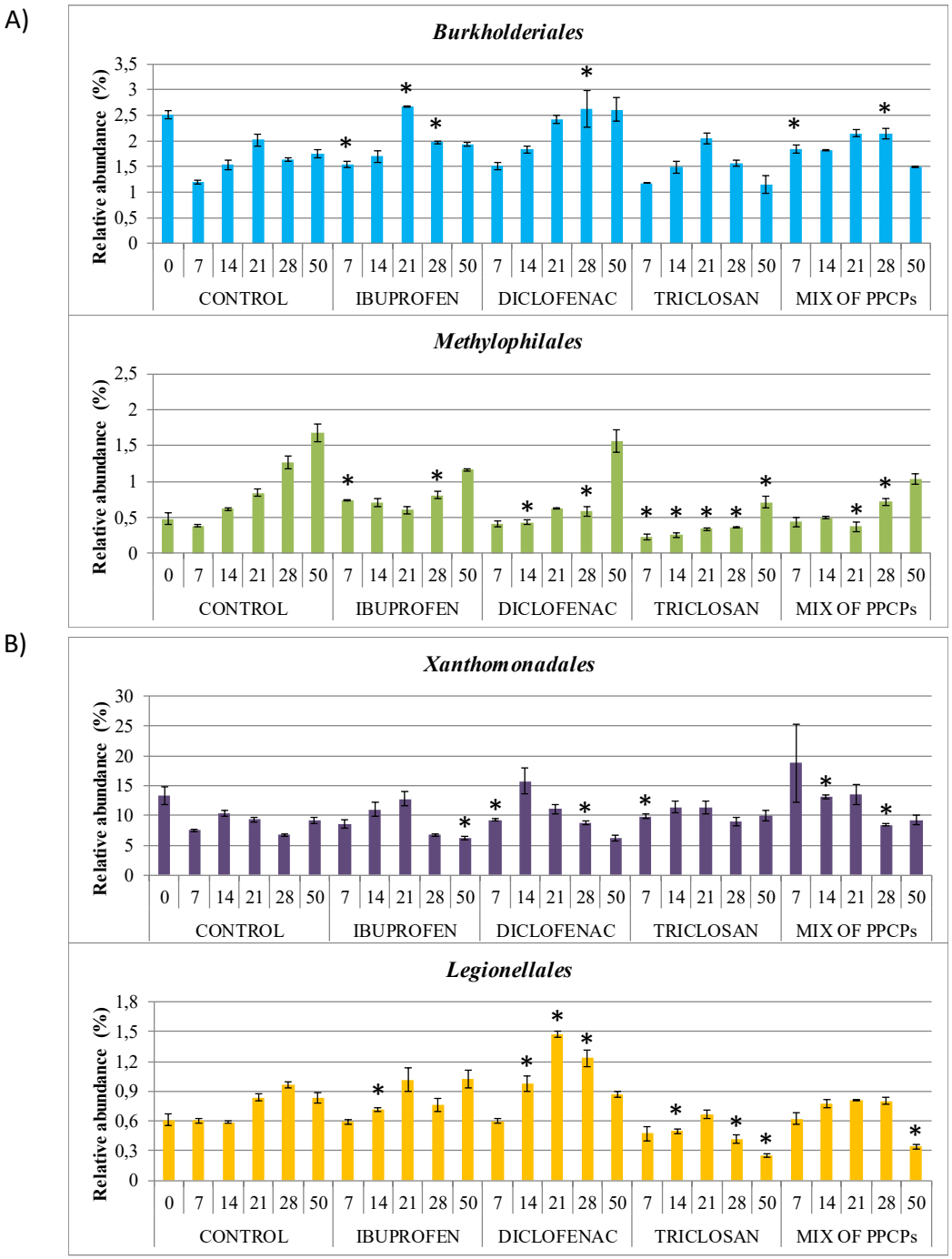

Figure S3. Relative abundance of different orders within the classes *Betaproteobacteria* (A) and *Gammaproteobacteria* (B). *Significant differences among non-contaminated (control) and contaminated BPS samples with ibuprofen, diclofenac and triclosan, applied separately and in mixture (ANOVA homogeneity test; $p < 0.05$). Error bars represent the standard error for each sample (n=3).

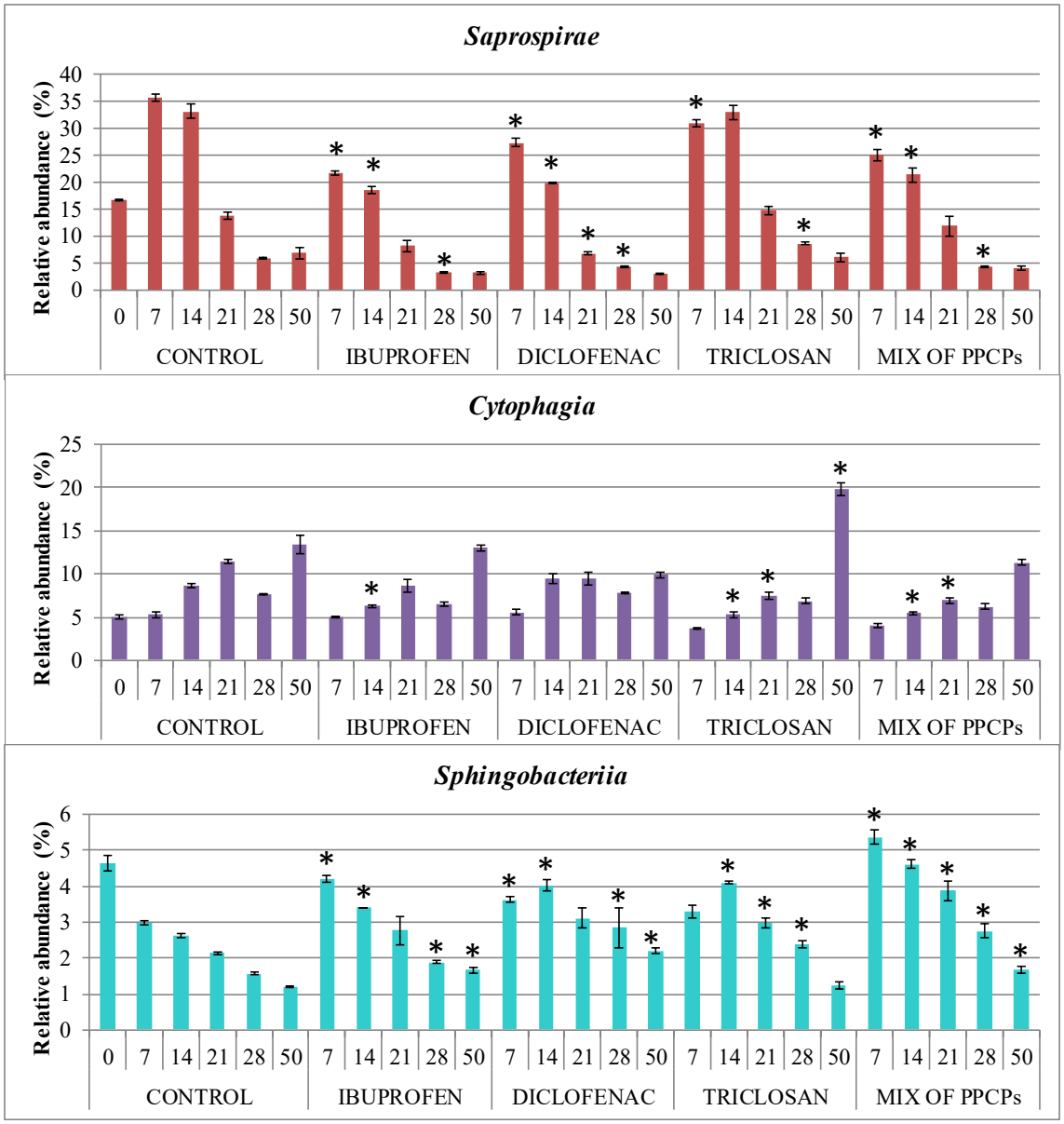

Figure S4. Relative abundance of the most representative classes within the phylum *Bacteroidetes*. *Significant differences among non-contaminated (control) and contaminated BPS samples with ibuprofen, diclofenac and triclosan, applied separately and in mixture (ANOVA homogeneity test; $p < 0.05$). Error bars represent the standard error for each sample (n=3).

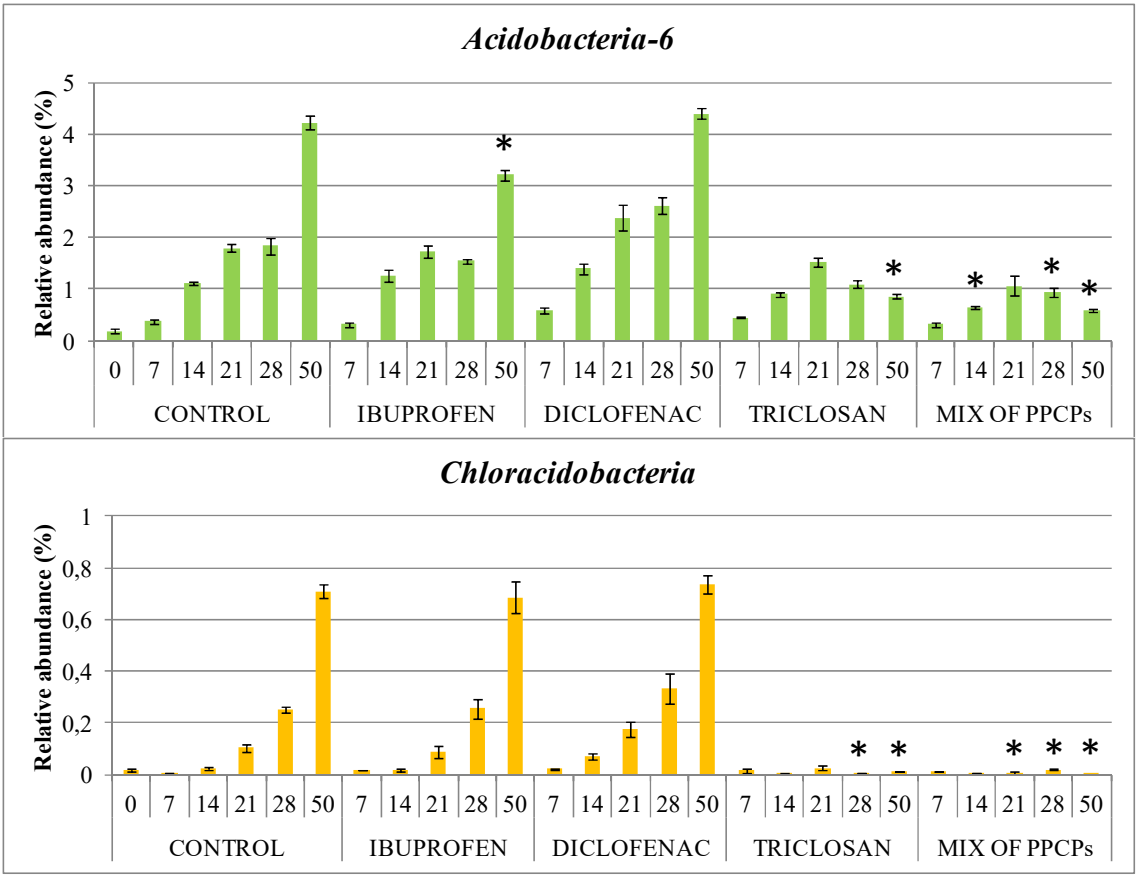

836

837 Figure S5. Relative abundance the most representative classes within the phylum
838 *Acidobacteria*. *Significant differences among non-contaminated (control) and
839 contaminated BPS samples with ibuprofen, diclofenac and triclosan, applied separately
840 and in mixture (ANOVA homogeneity test; $p < 0.05$). Error bars represent the standard
841 error for each sample (n=3).

842

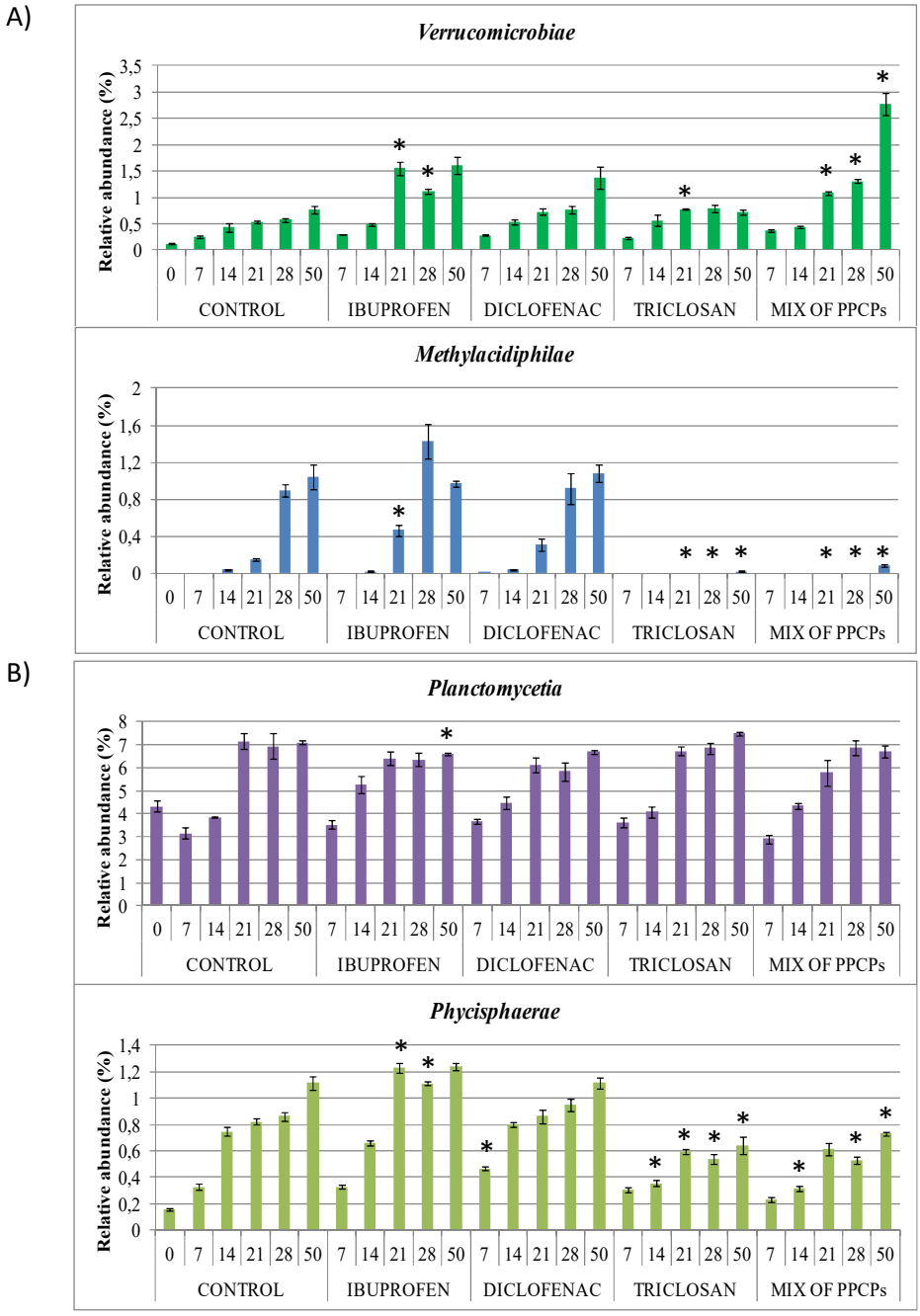

Figure S6. Relative abundance the most representative classes within the phyla *Verrumicrobia* (A) and *Planctomycetes* (B). *Significant differences among non-contaminated (control) and contaminated BPS samples with ibuprofen, diclofenac and triclosan, applied separately and in mixture (ANOVA homogeneity test; $p < 0.05$). Error bars represent the standard error for each sample (n=3).

Table S1. Gene copy number per nanogram of DNA of the different taxa from non-contaminated (control) and contaminated BPS samples with ibuprofen, diclofenac and triclosan, applied separately and in mixture at 0, 7 and 50 days of the incubation period. Standard errors (in parentheses) are given. Letters indicate significant differences among samples of different incubation times of each treatment and taxa (ANOVA homogeneity test; $p < 0.05$).

		Taxa				
Treatment	**Days**	**Total bacteria**	***α-Proteobacteria***	***β-Proteobacteria***	***γ-Proteobacteria***	***Acidobacteria***
	0	2.93×10^{5} (0.65)a	1.92×10^{5} (0.42)a	1.73×10^{3} (0.57)a	1.47×10^{5} (0.53)a	1.12×10^{3} (0.34)a
Control	7	7.28×10^{5} (1.05)a	4.08×10^{5} (0.76)a	9.35×10^{3} (2.14)a	3.27×10^{5} (0.32)a	1.56×10^{4} (0.26)a
	50	5.16×10^{5} (0.35)a	3.03×10^{5} (0.19)a	7.47×10^{3} (2.25)a	9.18×10^{4} (2.46)a	5.84×10^{4} (1.07)b
Ibuprofen	7	1.06×10^{6} (0.01)b	1.93×10^{5} (0.50)a	3.30×10^{3} (0.25)a	2.39×10^{5} (0.23)a	5.27×10^{3} (1.27)a
	50	4.65×10^{5} (0.34)a	3.11×10^{5} (0.21)a	1.26×10^{4} (0.01)b	1.44×10^{5} (0.06)a	7.37×10^{4} (0.29)b
Diclofenac	7	9.05×10^{5} (0.10)b	2.64×10^{5} (0.17)a	2.01×10^{3} (0.04)a	1.26×10^{5} (0.27)a	2.85×10^{3} (0.34)a
	50	5.44×10^{5} (0.09)a	3.92×10^{5} (0.28)a	1.73×10^{4} (0.31)b	1.65×10^{5} (0.04)a	8.84×10^{4} (0.82)b
Triclosan	7	1.19×10^{6} (0.12)b	3.76×10^{5} (0.78)a	1.06×10^{4} (0.57)a	3.46×10^{5} (1.16)a	1.83×10^{4} (0.69)a
	50	4.93×10^{5} (0.15)a	3.90×10^{5} (0.32)a	1.07×10^{4} (0.07)a	1.95×10^{5} (0.21)a	2.46×10^{4} (0.29)a
Mix	7	6.41×10^{5} (0.57)a	3.34×10^{5} (0.26)a	4.78×10^{3} (0.33)a	1.83×10^{5} (0.06)a	1.82×10^{4} (0.37)a
	50	5.05×10^{5} (0.47)a	2.72×10^{5} (0.24)a	5.04×10^{3} (1.08)a	1.34×10^{5} (0.34)a	1.18×10^{4} (0.22)a